

Pulse Duration Dependence of Infrared Laser-Induced Secondary Electron Yield Reduction of Copper Surfaces

Pierre Lorenz^{*1}, Elena Bez^{2,3}, Marcel Himmerlich², Martin Ehrhardt², Mauro Taborelli², and Klaus Zimmer^a

¹Leibniz Institute of Surface Engineering (IOM), Permoserstr. 15, D-04318 Leipzig, Germany

²CERN (European Organization for Nuclear Research), 1211 Geneva 23, Switzerland

³Faculty of Physics and Earth Sciences, University of Leipzig, Linnéstr. 5, 04103 Leipzig, Germany

*Corresponding author's e-mail: pierre.lorenz@iom-leipzig.de

The irradiation of metals with ultrashort laser pulses enables the rapid and cost-effective production of nanostructured surfaces with a wide range of industrial applications. The laser-induced surface roughening modifies the interaction processes upon electron impact, leading to a modification of the secondary electron emission. In this study, the nanostructuring as well as the secondary electron yield (SEY) variation of polycrystalline copper surfaces was investigated by irradiation with 1030 nm infrared ultrashort laser pulses at a constant repetition rate of 100 kHz. The influence of varying the pulse duration between 238 fs and 10 ps, the laser power and the number of laser pulses per unit area (induced by varying the scanning speed) on the surface topography and the SEY was investigated. Irrespective of the pulse duration, irradiation with low scan speed ($v \leq 20$ mm/s) and high laser power ($P \geq 2.6$ W) results in the formation of a surface with compact nanostructures and a very low maximum SEY $\delta_{\max} < 0.7$. The δ_{\max} increased slightly with increasing pulse duration at similar laser parameters. Increasing the pulse duration also resulted in a slight decrease in the ablation threshold and volume. The observed SEY dependence is probably explained by the pulse duration dependence of the ablation. The results suggest that nanostructured copper surfaces with very low SEY can be produced with ultrashort laser pulses over a wide range of pulse durations.

DOI: 10.2961/jlmn.2023.03.2002

Keywords: laser; SEY, copper, nanostructuring, pulse duration

1. Introduction

Short and ultrashort laser pulses can be used to create nanostructures on copper surfaces. Such micro-nanostructured surfaces exhibit interesting macroscopic properties, including reduced reflectivity [1] and reduced secondary electron yield (SEY) [2]. The SEY is defined as the number of secondary electrons emitted per incident electron and depends on the energy of the incident primary electrons. SEY engineering plays an important role in overcoming the performance limit of particle accelerators with intense positively charged beams [3-5]. The interaction of ultrashort laser pulses with copper surfaces has been extensively studied for different pulse durations and laser wavelengths. The studies have mainly focused on laser ablation processes in the nanosecond to femtosecond pulse duration range, with wavelengths from the ultraviolet to the infrared [3, 6-26]. Various parameters such as the number of laser pulses [6], the laser pulse energy [7], the repetition rate [8, 27], the gaseous environment [9, 10] and the presence of external magnetic fields affect the copper ablation process [11]. Multi-pulse burst irradiation has also been investigated [12, 28]. Ablation quantities such as the depth, the width, the shape and the volume of the formed craters and trenches depend

on the laser parameters [25]. In general, the ablation volume increases with increasing laser pulse energy and ultraviolet laser pulses are more effective for copper ablation than infrared laser pulses [7]. Laser ablation not only results in the removal of material, but a fraction of the ejected metal particles redeposit on the irradiated sample surface, either directly in the reaction zone of the laser focus or in nearby regions. This results in the formation of copper nanostructures on the treated surface, the morphology of which depends on the laser processing parameters [29]. This nanoparticle redeposition has many similarities to the widely studied pulsed laser deposition (PLD) process, which allows the deposition of thin films with complex stoichiometry. It is typically performed at low pressure for high quality film growth, and copper PLD has been studied under vacuum and ambient pressure conditions [30, 31]. In addition to nanostructuring, laser induced periodic surface structures (LIPSS) on copper also allow the adjustment of the SEY [32]. This study focuses on infrared ultrashort pulse laser treatment of copper surfaces as a function of pulse duration in air to achieve nanostructuring of copper surfaces with a reduced SEY of less than 1.

$$\Phi_{acc,A} = N_A \cdot \frac{P}{f_{rep} \cdot \pi \cdot \omega_0^2} = \frac{P}{v \cdot \Delta y} \quad (4)$$

2. Experimental Setup

The surface nanostructuring of cleaned, degreased, and subsequently passivated polycrystalline copper samples (size 20 x 20 x 1 mm³) was performed by laser irradiation using ultra-short laser pulses with a pulse duration between 238 fs and 10 ps. The samples were mounted onto an x-y-stage of a laser workstation and irradiated in air by a solid-state laser (Carbide CB3-40W from Light Conversion) with a laser wavelength of $\lambda = 1030$ nm and a variable pulse duration. The repetition rate was set to $f_{rep} = 100$ kHz. The laser beam with a Gaussian beam profile ($M^2 = 1.1$) was focused by a f-theta lens on the sample surface with a focal length of 165 mm. The Gaussian radius was determined by Liu plot, see section 3.1. Two different kinds of structuring processes were performed: engraving of single lines and areal treatments with overlapping lines.

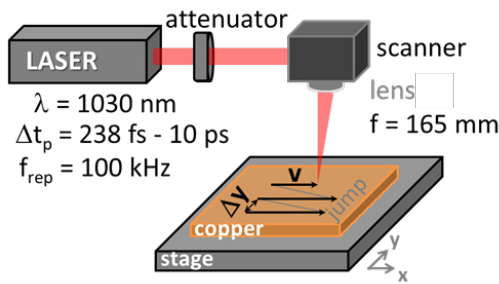


Fig. 1 Schematic illustration of the laser structuring setup.

For the single line processing, the focused laser beam was scanned by a galvo-scanner in geometrically separated parallel lines across the copper surface with a scanning velocity v that varied between 1 and 200 mm/s (see Fig. 1).

The accumulated number of laser pulses N_L for a single line is dependent on the Gaussian radius ω_0 , the repetition rate as well as the scanning speed:

$$N_L = \frac{f_{rep} \cdot 2 \cdot \omega_0}{v} \quad (1)$$

and the accumulated laser fluence $\Phi_{acc,L}$ can be calculated by:

$$\Phi_{acc,L} = N_L \cdot \frac{P}{f_{rep} \cdot \pi \cdot \omega_0^2} = \frac{2 \cdot P}{v \cdot \pi \cdot \omega_0} \quad (2)$$

For the areal processing, homogeneously structured copper surfaces were fabricated with partial overlap of the scanned lines for a total treated area of 18 x 18 mm² per sample (see Fig. 1). The line distance was set to $\Delta y = 50$ μ m. For overlapping lines, the accumulated number of laser pulses N_A can be estimated by:

$$N_A = \frac{f_{rep} \cdot \pi \cdot \omega_0^2}{v \cdot \Delta y} \quad (3)$$

With the accumulated number N_A of laser pulses, the accumulated laser fluence Φ_{acc} is given by:

The separated lines were measured by white light interferometry (WLI), in particular the ablated volume V_{ab} , the line diameter d and the line depth Δz were analyzed. The ablation volume per laser pulse was estimated from the ablated volume V_{ab} at a line length equal to twice the Gaussian radius ω_0 divided by the number of laser pulses N_L (Eq. 1). Before the measurement, the lines were mechanically wipe-cleaned using propanol-immersed cotton and subsequently underwent ultrasonication in propanol to remove any re-deposited material and particles inside the trenches.

For the samples that underwent large-area processing, the surface topography was measured by optical microscopy (OM) and scanning electron microscopy (SEM) and the secondary electron yield (SEY) was measured for primary electron energies between 50 and 1800 eV [3].

3. Experimental results and Discussion

3.1 Ablation characteristics in dependence of pulse duration

In Fig. 2 (a), the square of the line width in dependence of the natural logarithmic of the laser power at fixed scanning speed of 2 mm/s is shown for selected pulse durations (Liu plot [33]). All lines are almost parallel. From the slope, the Gaussian radius was determined to be (23 ± 0.5) μ m. Based on the estimated Gaussian radius, a laser pulse number $N_L = 2300$ was calculated for $v = 2$ mm/s. Further, the ablation threshold P_{th} in dependence of the pulse duration can be calculated from the extrapolation at $d=0$ for the given conditions of at $N_L = 2300$ (see Fig. 2 (b)). The ablation threshold at $N_L = 2300$ slightly increases for increasing pulse duration from ~ 0.21 W ($\Phi_{th} \sim 130$ mJ/cm²) at $\Delta t_p = 238$ fs to ~ 0.28 W ($\Phi_{th} \sim 170$ mJ/cm²) at 10 ps. The obtained values are in the expected order of magnitude and are in reasonable agreement with previously reported values [34-36]. For example Chen et al. [36] reported a single pulse ablation threshold of 0.6 J/cm² at $\Delta t_p = 1$ ps. Furthermore, the ablation volume per laser pulse V_N was determined as a function of the pulse duration. The change of V_N for a treatment at an average laser power of $P = 4.33$ W ($\Phi = 2.6$ J/cm² for a single pulse) and $v = 2$ mm/s ($\Phi_{acc,L} \sim 6$ kJ/cm²) is summarized in Fig. 2 (c). The increase of the pulse duration resulted in a slight decrease of the ablation volume, in consistence with the increase in P_{th} . The ablation volume per laser pulse decreased from ~ 17 μ m³ (ablation volume per laser pulse and pulse energy: 0.4 μ m³/ μ J) at $\Delta t_p = 238$ fs to ~ 14 μ m³ (0.32 μ m³/ μ J) at 10 ps. The determined ablation volume of this study is slightly smaller than the value published by Zemaitis et al. [12] and the dependence on pulse duration is inverted. These discrepancies are attributed to the difference in the utilized laser parameter during treatment (scanning speed, repetition rate, Gaussian radius, laser power).

3.2 Surface topography and nanostructure formation in dependence of pulse duration

The laser irradiation results in a modification of the copper surface, which strongly depends on the different processing parameters (see Figs. 3 and 4).

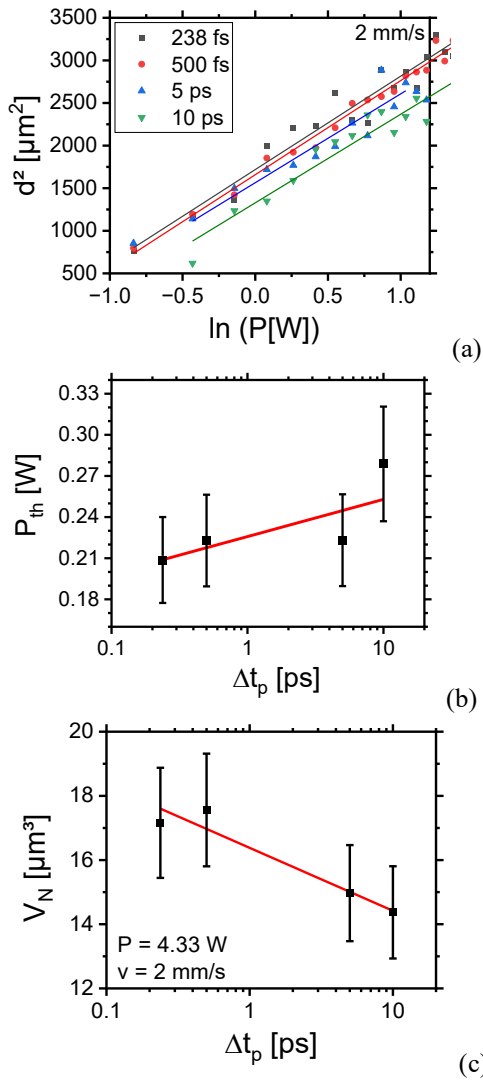


Fig. 2 (a) Liu plot of laser treated lines in copper at a scanning speed of $v = 2 \text{ mm/s}$ ($N_L = 2300$) at different pulse duration. For better readability of the graph, the error bars are not shown ($\Delta d \sim 2 \mu\text{m}$). (b) Ablation threshold P_{th} dependence on the pulse duration (red line: trend line guide for the eye). (c) Ablation volume per laser pulse V_N in dependence of the pulse duration at constant average laser power $P = 4.33 \text{ W}$ and $v = 2 \text{ mm/s}$ (red line: trend line guide for the eye).

The irradiation with high laser power and low scanning speed results in the formation of compact nanostructures, independent of the pulse duration. The parameter range, which results in the formation of compact nanostructures, is marked red in Fig. 3 and Fig. 4.

At short pulse duration, the necessary laser power for the formation of compact nanostructures is smaller than for longer pulses (see Fig. 3 and 4). For example, at fixed scan speed of 20 mm/s , for 500 fs pulses a laser power of $\sim 2.6 \text{ W}$ is necessary, while at 10 ps pulses a power of $\sim 3.46 \text{ W}$ is required.

The increase of the onset of nanostructure formation for larger pulse duration follows the trend that the ablation threshold increases at the same time (see Fig. 2 (b)). Furthermore, at low laser power and high scanning speed, the laser treatment induces no or only minor changes to the surface topography. The parameter field is marked green in Figs. 3

and 4. In accordance with the ablation threshold dependency, the parameter field, for which no or only minor changes occur, is narrower at low pulse duration (500 fs) than at long pulse duration (10 ps).

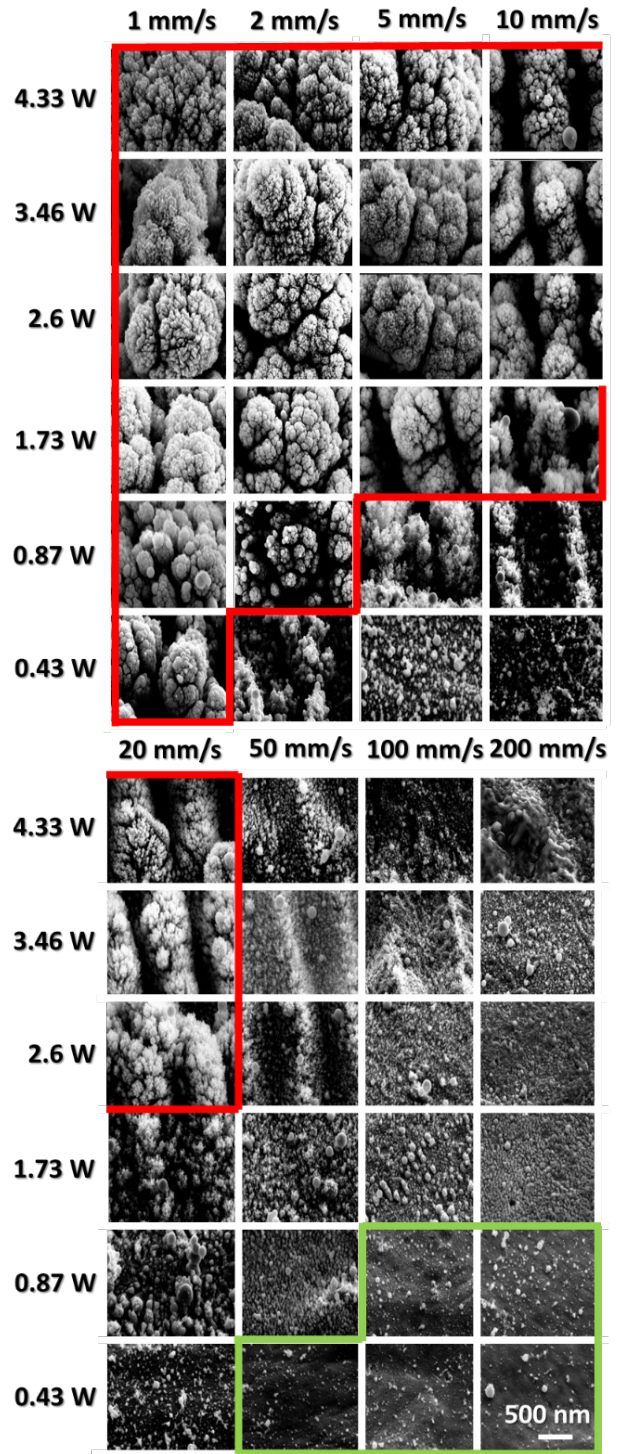


Fig. 3 Scanning electron micrographs of copper surfaces after treatment with different laser power and scanning speed (as indicated) at a pulse duration of $\Delta t_p = 500 \text{ fs}$.

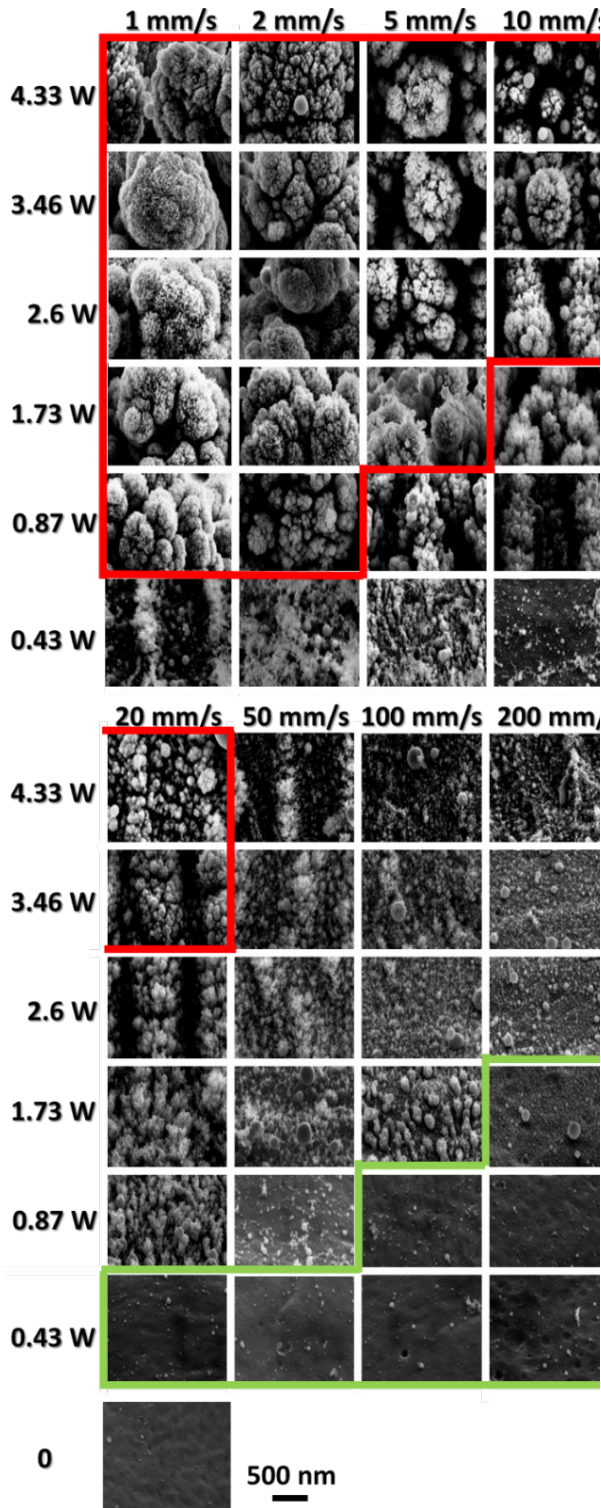
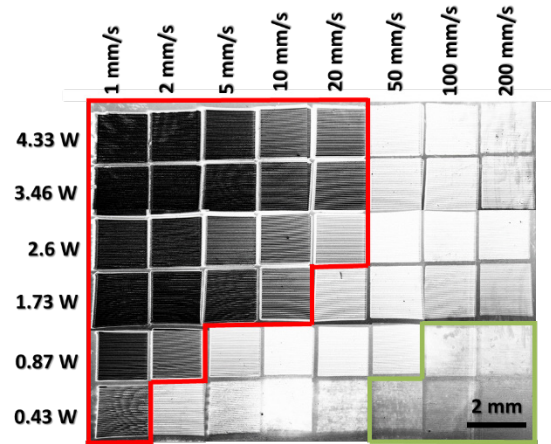


Fig. 4 Scanning electron micrographs of copper surfaces after treatment with different laser power and scanning speed (as indicated) at a pulse duration of $\Delta t_p=10$ ps.

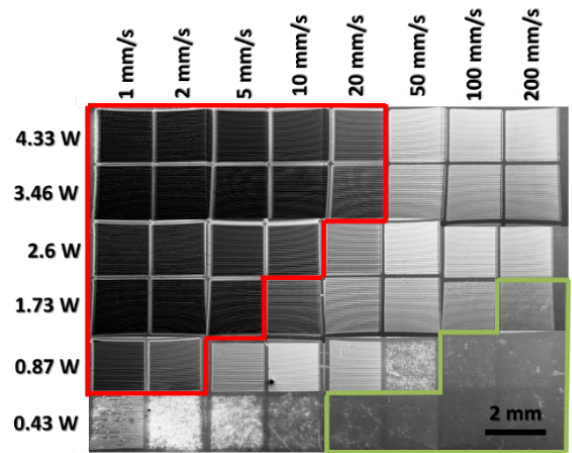
3.3 Secondary Electron Yield

Besides the high-resolution SEM images, also low-resolution SEM images were acquired at a primary electron energy of 5 keV and fixed detector settings. In Fig. 5 such scanning electron micrographs are shown for which the brightness allows a qualitative assessment of the number emitted secondary electrons at 5 keV, i.e. areas with a reduced secondary

electron emission appear dark and areas with increased secondary electron emission appear bright. The picture clearly shows that the variation in laser processing parameters has an influence on the secondary electron emission. Especially the compact nanostructures exhibit a reduced secondary electron emission, while an intermediate fluence during treatment increases the electron emission at 5 keV compared to untreated copper.



(a) $\Delta t_p = 500$ fs



(b) $\Delta t_p = 10$ ps

Fig. 5 Secondary electron low resolution SEM images at a primary electron energy of 5 keV for samples treated with different laser power and scanning speed (as indicated) at pulse durations of $\Delta t_p = 500$ fs (a) and $\Delta t_p = 10$ ps (b)

The secondary electron yield (SEY) in the primary electron energy range between 50 and 1800 eV for selected samples treated at high power and slow scanning speed ($P = 4.33$ W, $v = 2$ mm/s) is shown in Fig. 6 (b). At low pulse duration ($\Delta t_p = 500$ fs) and high pulse duration ($\Delta t_p = 10$ ps) the irradiation results in a distinct reduction of the SEY compared to an untreated copper surface, which exhibits a maximum secondary electron yield of $\delta_{max} = 2.2$ [20]. The SEY maximum of the laser treated surfaces increased at increasing primary electron energy up to a primary electron energy of $E_p \sim 1300$ eV to $\delta_{max} \sim 0.63$ and ~ 0.69 at $\Delta t_p = 500$ fs and 10 ps, respectively.

In Fig 6 (c) the secondary electron yield maximum of the laser treated copper surfaces in dependence of the pulse du-

ration is summarized including the variation across the samples as indicated by the error bars. There is a tendency for the δ_{\max} to increase slightly with increasing pulse duration. The maximum absolute error of our SEY measurement is 0.05 - 0.1 for $\delta < 0.8$. Consequently, the difference between the samples is not significant. Nonetheless, the slight trend can be understood considering the similar surface structures that are formed for 500 fs and 10 ps pulse duration (see Fig. 6 (a)) via partial redeposition of copper nanostructures from the ablated material in the generated plasma plume [20].

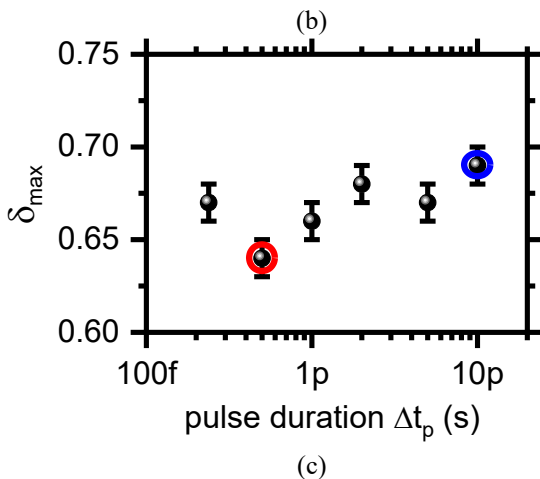
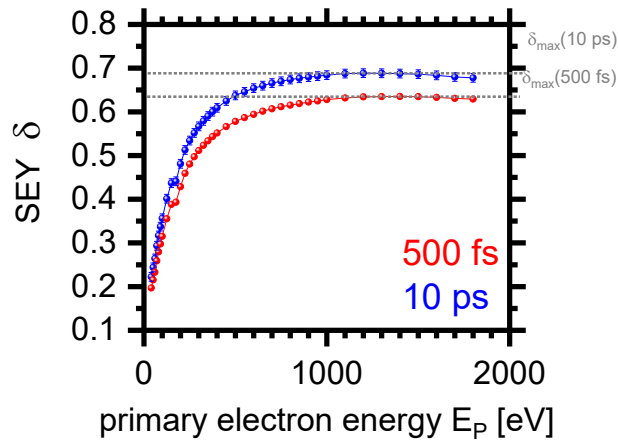
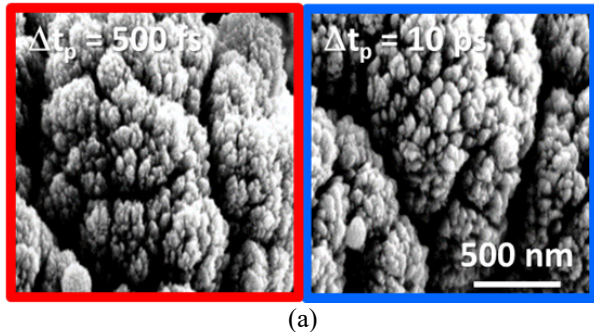


Fig. 6 (a) High resolution scanning electron micrographs of copper surfaces after laser treatment ($P = 4.33$ W, $v = 2$ mm/s) with pulse durations of $\Delta t_p = 500$ fs (left, red marked) or 10 ps (right, blue marked). (b) SEY in dependence of the primary electron energy for the same copper surfaces. (c) SEY maximum δ_{\max} in dependence of the laser pulse duration Δt_p utilized for surface processing. The error bars represent the standard deviation based on measurements at three different spots on each sample to evaluate sample homogeneity.

The SEY can vary if the surface composition changes. We have performed X-ray photoelectron spectroscopy analysis of the samples (not shown) using the same conditions as in Ref. [3]. Laser treatment in ambient air at high laser fluences > 2000 J/cm² leads to strong roughening, very low SEY and oxidation of particles in the reaction zone resulting in the formation of a CuO-like surface [3]. The XPS results of the samples discussed in this study are identical to these earlier observations. Furthermore, the surface composition did not change when the pulse duration was varied. Consequently, the changes in SEY can be attributed to topographic variations. In general, δ_{\max} increases for increasing accumulated laser fluence and the ablation volume / nanostructured layer thickness increases at increasing accumulated laser fluence [3, 20-22]. The experimental results in the literature suggest that the resulting SEY depends, among other influences, on the density of the nanoparticles on the surface, i.e. the SEY decreases with increasing particle density. The performed line tests revealed that the ablation volume slightly decreases for increasing pulse duration, which is expected to lead to a lower particle density on the processed surface, and thus to slightly influence on the SEY.

4. Conclusions

IR laser irradiation of polycrystalline copper with ultra-short laser pulses allows the fabrication of micro/nanostructured surfaces at different pulse durations Δt_p from 238 fs to 10 ps. The nanostructured surface, especially the compact nanostructures generated at high laser power and low scan speed, results in a very low secondary electron yield (SEY) maximum of only 0.63. The SEY maximum increases slightly with increasing pulse duration (at constant laser power or accumulated laser fluence, where the pulse peak intensity is reduced), while the shape of the nanostructures formed is similar. The slight increase of δ_{\max} can be explained by the reduction of the ablation volume by more than 20%, resulting in fewer deposited nanoparticles. The laser-based SEY modification can be extended to other materials.

References

- [1] B. Hopp, T. Smausz, M. Lentner, J. Kopniczky, C. Tápai, T. Gera, T. Csizmadia, M. Ehrhardt, P. Lorenz, and K. Zimmer: Appl. Phys. A, 123, (2017) 598.
- [2] D. Bajek, S. Wackerow, D.A. Zanin, L. Baudin, K. Bogdanowicz, E.G.-T. Valdivieso, S. Calatroni, B. Di Girolamo, M. Sitko, M. Himmerlich, M. Taborelli, P. Chiggiato, and A. Abdolvand: Sci Rep, 10, (2020) 250.
- [3] E. Bez, M. Himmerlich, P. Lorenz, M. Ehrhardt, A.G. Gunn, S. Pfeiffer, M. Rimoldi, M. Taborelli, K. Zimmer, P. Chiggiato, and A. Anders: J. Appl. Phys., 133, (2023) 035303.
- [4] C. Yin Vallgren, G. Arduini, J. Bauche, S. Calatroni, P. Chiggiato, K. Cornelis, P.C. Pinto, B. Henrist, E. Métral, H. Neupert, G. Rumolo, E. Shaposhnikova, and M. Taborelli: Physical Review Special Topics - Accelerators and Beams, 14, (2011) 071001.
- [5] W. Vollenberg, P. Costa Pinto, P. Chiggiato, P. Cruikshank, H. Moreno, C. Pasquino, M. Taborelli, and J. Perez Espinos: JACoW IPAC, 2021, (2021) 3475.
- [6] H. Büttner, M. Hajri, R. Roth, and K. Wegener: Procedia CIRP, 68, (2018) 190.
- [7] L. Tunna, A. Kearns, W. O'Neill, and C. J. Sutcliffe: Opt. Laser Technol., 33, (2001).
- [8] J. Schille, L. Schneider, L. Hartwig, U. Loeschner, R. Ebert, P. Scully, N. Goddard, and H. Exner: International Congress on Applications of Lasers & Electro-Optics, 2012, (2012) 949.
- [9] A. Bogaerts, Z. Chen, and D. Bleiner: J. Anal. At. Spectrom., 21, (2006) 384.

- [10] T. Smausz, T. Csizmadia, C. Tápai, J. Kopniczky, A. Oszkó, M. Ehrhardt, P. Lorenz, and K. Zimmer, A. Prager, and B. Hopp: *Appl. Surf. Sci.* 389, (2016) 1113.
- [11] P.K. Pandey, S.L. Gupta, and R.K. Thareja: *Phys. Plasmas*, 22, (2015) 073301.
- [12] A. Žemaitis, P. Gečys, M. Barkauskas, G. Račiukaitis, and M. Gedvilas, *Sci Rep*, 9, (2019) 12280.
- [13] W. de Rossi, D. de Carmargo Mirim, N.D. Vieira Junior, and S.R. Elgul: *Lasers in Manufacturing Conference*, 2015 (2015).
- [14] R. Jordan, D. Cole, J.G. Lunney, K. Mackay, and D. Givord: *Appl. Surf. Sci.*, 86, (1995) 24.
- [15] A.N. Hannah, P. Krkotić, R. Valizadeh, O.B. Malyshev, J. Mutch, D.J. Whitehead, M. Pont, J.M. O'Callaghan, and V. Dhanak: *Vacuum*, 189, (2021) 110210.
- [16] R. Valizadeh, O.B. Malyshev, S. Wang, T. Sian, M.D. Cropper, and N. Sykes: *Appl. Surf. Sci.*, 404, (2017) 370.
- [17] D.A. Zayarny, A.A. Ionin, S.I. Kudryashov, S.V. Makarov, A.A. Kuchmizhak, O.B. Vitrik, and Y.N. Kulchin: *Laser Phys. Lett.*, 13, (2016) 076101.
- [18] J. Yang, Y. Zhao, N. Zhang, Y. Liang, and M. Wang: *Phys. Rev. B*, 76, (2007) 165430.
- [19] J. Mur, J. Petelin, N. Osterman, and R. Petkovšek: *J. Phys. D*, 50, (2017) 325104.
- [20] P. Lorenz, M. Himmerlich, M. Ehrhardt, E. Bez, K. Bogdanowicz, M. Taborelli, and K. Zimmer: *Lasers Manuf. Mater.*, 9, (2022) 135.
- [21] P. Lorenz, E. Bez, M. Himmerlich, M. Ehrhardt, M. Taborelli, and K. Zimmer: *Procedia CIRP*, 111, (2022) 662.
- [22] P. Lorenz, M. Himmerlich, M. Ehrhardt, E. Bez, K. Bogdanowicz, M. Taborelli, and K. Zimmer: *Proc. SPIE*, Vol. 11989, (2022) 119890A.
- [23] H. Nicolai, M. Stolze, T. Herrmann, and J.A. Lhuillier: *Proc. SPIE*, Vol. 9351, (2015) 93510E.
- [24] M. Hashida, A.F. Semerok, O. Gobert, G. Petite, Y. Izawa, and J.F. Wagner: *Appl. Surf. Sci.*, 197-198, (2002) 862.
- [25] J. Schille, L. Schneider, P. Lickschat, U. Loeschner, R. Ebert, and H. Exner: *J. Laser Appl.*, 27, (2015) S28007.
- [26] A. Abdelmalek, Z. Bedrane, E.-H. Amara, B. Sotillo, V. Bharadwaj, R. Ramponi, and S.M. Eaton: *Appl. Sci.*, 8, (2018) 1826.
- [27] J. Lopez, Y. Zaouter, R. Torres, M. Faucon, C. Hönninger, P. Georges, M. Hanna, E. Mottay, and R. Kling: *International Congress on Applications of Lasers & Electro-Optics*, 2013, (2013) 686.
- [28] B. Bornschlegel and J. Finger: *J. Laser Micro/Nanoeng.*, 14, (2019) 7.
- [29] P.X. Fan, M.L. Zhong, L. Li, P. Schmitz, C. Lin, J.Y. Long, and H.J. Zhang: *J. Appl. Phys.*, 115, (2014) 13.
- [30] M.R. Rashidian Vaziri and F. Hajiesmaeilbaigi: *Optik*, 126, (2015) 1348-1351.
- [31] M. Fernández-Arias, M. Boutinguiza, J. Del Val, A. Riveiro, D. Rodríguez, F. Arias-González, J. Gil, and J. Pou: *Nanomaterials* 10, (2020) 300.
- [32] J. J. Nivas, M. Hu, M. Valadan, M. Salvatore, R. Fittipaldi, M. Himmerlich, E. Bez, M. Rimoldi, A. Passarelli, S.L. Oscurato, A. Vecchione, C. Altucci, S. Amoroso, A. Andreone, S. Calatroni, and M. Rosaria Masullo: *Appl. Surf. Sci.*, 622, (2023) 156908.
- [33] J.M. Liu: *Opt. Lett.*, 7, (1982) 196.
- [34] G. Raciukaitis, M. Brikas, P. Gečys, B. Voisiat, and M. Gedvilas: *J. Laser Micro/Nanoeng.*, 4, (2009) 186.
- [35] R. Uren, A. Din, S. Wackerow, E. Bez, S. Pfeiffer, M. Rimoldi, M. Himmerlich, M. Taborelli, and A. Abdolvand: *Opt Mater Express*, 13 (2023) 1228-1240.
- [36] C.-W. Cheng and J.-K. Chen: *Appl. Phys. A*, 126, (2020) 649.

(Received: June 14, 2023, Accepted: September 30, 2023)